DALTON
FULL PAPER

Synthesis and DNA binding properties of bioorganometallic (η^5-pentamethylcyclopentadienyl)iridium(III) complexes of the type $[(\eta^5\text{-}C_5Me_5)Ir(Aa)(dppz)]^{n+}$ (dppz = dipyrido[3,2-*a*:2′,3′-*c*]-phenazine, *n* = 1–3), with S-coordinated amino acids (Aa) or peptides

Diran Herebian and William S. Sheldrick

Lehrstuhl für Analytische Chemie, Ruhr-Universität Bochum, D-44780 Bochum, Germany

Received 23rd August 2001, Accepted 12th December 2001
First published as an Advance Article on the web 21st February 2002

The DNA binding of cationic complexes of the type $[(\eta^5\text{-}C_5Me_5)Ir(Aa)(dppz)](CF_3SO_3)_n$ (dppz = dipyrido[3,2-*a*:2′,3′-*c*]-phenazine; *n* = 1, Aa = AccysOH **7**; *n* = 2, Aa = AcmetOMe **4**, H_2cysOMe **8**; *n* = 3, Aa = H_2metOMe **5**) containing S-coordinated amino acids (HmetOH = methionine, HcysOH = cysteine) has been studied by UV-vis titration, 2D-NOESY and gel electrophoresis. The observed steady decrease in absorbance at maxima between 350 and 400 nm on UV-vis titration with CT DNA and the bathochromic shifts of these absorption maxima are consistent with stable intercalative DNA binding for these complexes. An increase in the binding constant K_b from $8.80(6) \times 10^4$ for the monocation of **7** through $2.30(4) \times 10^5$ and $7.04(5) \times 10^5$ for the dications of **8** and **4** to $2.62(3) \times 10^6$ M^{-1} for the 3+ cation of **5** clearly reflects the strengthening of the electrostatic interaction with the negatively charged phosphodiester backbone of DNA with increasing cation charge. Analogous values of $2.81(7) \times 10^5$ and $1.26(5) \times 10^6$ M^{-1} were obtained for the $(\eta^5\text{-}C_5Me_5)Rh^{III}$ complexes **14** (*n* = 2, Aa = H_2cysOMe) and **13** (*n* = 3, Aa = H_2metOMe). Binding site sizes for the organometallic Ir^{III} and Rh^{III} complexes on CT DNA lie in the range 1.5–2.1 base pairs. NOE cross peaks for the 1 : 1 complex formed between **5** and $d(GTCGAC)_2$ are consistent with intercalation adjacent to T_2 from the major groove. Complexes **4**, **5** and $[(\eta^5\text{-}C_5Me_5)Ir(HglyglymetOH)(dppz)](CF_3SO_3)_2$ **6** (HglyOH = glycine) cleave the supercoiled plasmid *pBluescript II KS*+, on irradiation for 30–180 s with a high pressure Hg lamp, to afford nicked circular and linear DNA forms. X-Ray structural analyses are reported for $[(\eta^5\text{-}C_5Me_5)IrCl(dppz)](CF_3SO_3)$ **3** and $[(\eta^5\text{-}C_5Me_5)Ir(9\text{-Etgua})(phen)](CF_3SO_3)_2$ **16** (9-Etgua = 9-ethylguanine).

Introduction

The intercalation of transition metal polypyridyl complexes such as $[Ru(bpy)_2(dppz)]^{2+}$ (bpy = 2,2′-bipyridine, dppz = dipyrido[3,2-*a*:2′,3′-*c*]phenazine)[1] into DNA has been a topic of major bioinorganic interest in the past two decades.[2,3] In contrast, the low solubility and instability of many organometallic complexes in water appear to have discouraged analogous binding studies and it is only relatively recently that a report of DNA intercalation by a complex of this type, namely $[(\eta^5\text{-}C_5Me_5)Ru(dppz)(NO)](OTf)_2$, has appeared.[4] Interestingly the $(\eta^5\text{-}C_5Me_5)Ru^{II}$ fragment has also been employed to prepare chiral-at-metal α-amino acid (Aa) complexes,[5] as have the $(\eta^5\text{-}C_5Me_5)M^{III}$ (M = Rh, Ir) and $(\eta^6\text{-arene})Ru^{II}$ half-sandwich moieties.[6–10] The observed stability of such organometallic compounds in aqueous solution prompted us to synthesise potential intercalators of the type $[(\eta^5\text{-}C_5Me_5)M(Aa)(dppz)]^{n+}$ (*n* = 1–3), in which methionine- (met) or cysteine-containing (cys) amino acids (Aa) or tripeptides coordinate the Group 9 transition metal through the S atoms of their side chains. We reasoned that DNA binding of members of this new class of bioorganometallic complexes could be enhanced by additional electrostatic and/or hydrogen bonding interactions between the amino acid/peptide ligands and the biopolymer. For instance, tryptophan-containing peptides[11] and substituted naphthalene or quinoline systems[12] have been shown only to intercalate into double-stranded calf thymus DNA (CT DNA) when they bear positively charged ammonium groups in their side chains. Furthermore DNA site specificity has been found to depend on side-chain functional groups in a family of intercalators in which short oligopeptides were coupled to the phen′ ligand of $[Rh(phi)_2(phen')]^{3+}$ (phi = 9,10-phenanthrenequinone diimine, phen′ = 5-(amidoglutaryl)-1,10-phenanthroline).[13] Herein we now report the results of UV spectroscopic, NMR and gel electrophoretic studies of the binding of organometallic complexes of the type $[(\eta^5\text{-}C_5Me_5)Ir(Aa)(dppz)]^{n+}$ with CT DNA and plasmid *pBluescript II KS*+ (2958 bp, 50.2% GC base pairs). Two analogous $(\eta^5\text{-}C_5Me_5)Rh^{III}$ complexes with methionine methyl ester (H_2metOMe) and cysteine methyl ester (H_2cysOMe) as amino acid ligands were included for comparison purposes.

Results and discussion

The parent $(\eta^5\text{-}C_5Me_5)M^{III}$ complexes of the type $[(\eta^5\text{-}C_5Me_5)MCl(dppz)](CF_3SO_3)$ **3** (M = Ir) and **12** (M = Rh) were prepared by addition of the chelating ligand dppz to an acetone solution of $[(\eta^5\text{-}C_5Me_5)MCl(Me_2CO)_2](CF_3SO_3)$, obtained by precipitation of one half of the chloride ligands in $[(\eta^5\text{-}C_5Me_5)MCl_2]_2$ as AgCl. Fig. 1 depicts the X-ray structure of the monocation of **3**, in which the $C_5Me_5^-$ and dppz ligands exhibit an interplanar angle of 60.2(1)°. Ir–C distances to the cyclopentadienyl carbon atoms lie in the narrow range 2.181(3)–2.205(3) Å. As to be expected, the aromatic systems of neighbouring dppz ligands participate in π-stacking in the triclinic crystal lattice of **3**.

Bioorganometallic complexes containing respectively AcmetOMe (**4**), H_2metOMe (**5**, **13**), AccysOH (**7**) and H_2cysOMe (**8**, **14**) were obtained by direct reaction of the relevant starting

 DOI: 10.1039/b107656f

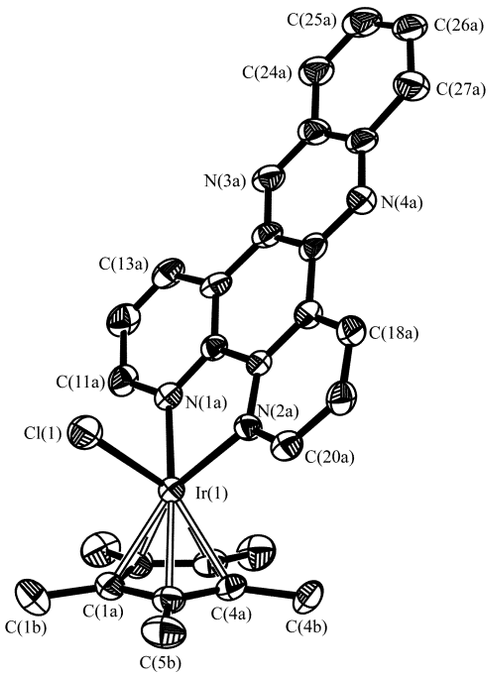

Fig. 1 Molecular structure of the cation of $[(\eta^5\text{-}C_5Me_5)Ir(Cl)(dppz)](CF_3SO_3)$ **3** with thermal ellipsoids given at 40% probability. Selected bond lengths (Å): Ir(1)–N(1a) 2.117(6), Ir(1)–N(2a) 2.083(6), Ir(1)–Cl(1) 2.398(2).

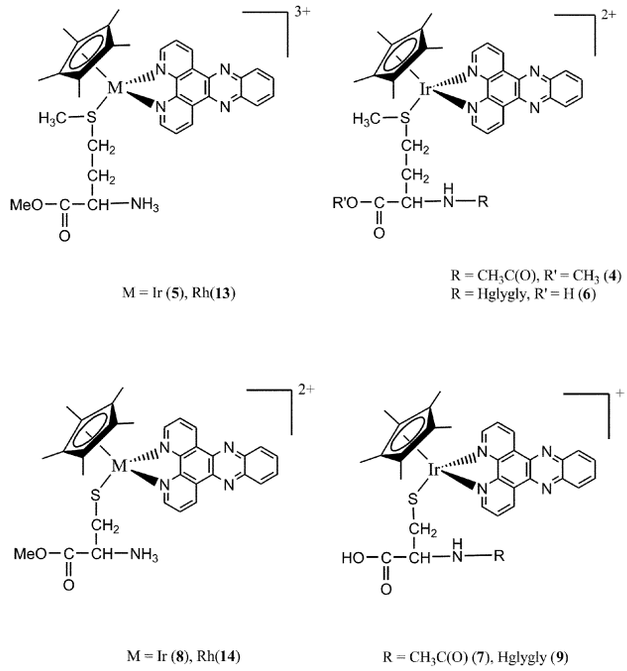

Scheme 1 Structural formulae of compounds **4**–**9**, **13** and **14**.

compound $[(\eta^5\text{-}C_5Me_5)M(Me_2CO)_3](CF_3SO_3)_2$ **1b** (M = Ir) or **2b** (M = Rh) with equivalent quantities of dppz and the methionine or cysteine derivative in a CH_3OH/CH_2Cl_2 solution at reflux. The analogous compounds $[(\eta^5\text{-}C_5Me_5)Ir(H_2metOMe)(phen)](CF_3SO_3)_3$ **10** and $[(\eta^5\text{-}C_5Me_5)Ir(H_2cysOMe)(phen)](CF_3SO_3)_2$ **11** were synthesized under similar conditions using (1,10)-phenanthroline (phen) as an alternative chelating ligand. To prevent competitive coordination of the non-protonated amino groups of the tripeptides HglyglymetOH and HglyglycysOH, these were added, following reaction of **1b** with dppz, in a second step together with 2 ml CF_3COOH during the preparation of $[(\eta^5\text{-}C_5Me_5)Ir(HglyglymetOH)(dppz)](CF_3SO_3)_2$ (**6**) and $[(\eta^5\text{-}C_5Me_5)Ir(HglyglycysOH)(dppz)](CF_3SO_3)$ (**9**). Compounds **4**–**11** and the analogous $(\eta^5\text{-}C_5Me_5)Rh^{III}$ derivatives **13** and **14** provide a series of potential cationic intercalators, whose differing total charges (n = 1–3) and charge distribution patterns (*i.e.* at the central metal atom and for **5**, **8**, **13** and **14** with an additional positively charged ammonium group) allow a systematic probing of the strength of DNA binding (Scheme 1).

All complexes were characterised by FAB mass spectrometry, ^{1}H and ^{13}C NMR, IR and UV-vis spectroscopy. Characteristic downfield ^{1}H NMR shifts of 0.10–0.15 ppm are observed for the Cp* methyl protons in **4**–**11** and **13**, **14** in comparison to the δ values of 1.74 and 1.75 for these singlets in the chloro complexes **3** and **12**. In contrast, the thioether δ-CH_3 protons adjacent to the coordinated sulfur atoms in the met-containing complexes **4**–**6**, **10** and **12** exhibit a somewhat more pronounced opposite shift from typical values of *ca.* 2.10 ppm in the free amino acids or peptides to the resonance positions in the range δ 1.84–1.90. This behaviour represents a striking reversal of the typical positive shift experienced by such methyl protons in analogous half-sandwich organometallic complexes without a chelating dppz or phen ligand.[5,7] The shielding cone of the adjacent dppz ligand could be responsible for this anomalous upfield shift.

Before turning in detail to DNA binding studies, it is important to consider the possible competition between intercalation and direct coordination by base nitrogen atoms for such bio-organometallic complexes. The kinetics of amino acid substitution by the model purine base 9-ethylguanine (9-Etgua) were, therefore, studied by ^{1}H NMR spectroscopy at pH 7.2 for complex **4**. Slow replacement of AcmetOMe by 9-Etgua leads to a steady increase of the Cp* resonance of $[(\eta^5\text{-}C_5Me_5)Ir(dppz)(9\text{-Etgua})](CF_3SO_3)_2$ **15** at δ 1.80 over a period of *ca.* 50 hours, a change that is accompanied by a concomitant reduction in the integral value of the Cp* signal for **4** at δ 1.89. As depicted in Fig. 2b, the equilibrium concentrations of both species are then present in a *ca.* 1 : 1 ratio. The ligand substitution involves initial slow dissociative loss of AcmetOMe followed by rapid coordination of the $(\eta^5\text{-}C_5Me_5)Ir^{III}$ fragment through N7 of 9-Etgua. A linear regression analysis of the time-dependence of the function $\ln[I_t(\mathbf{4})/I_o(\mathbf{4})]$, where I_o and I_t represent the integral values of the Cp* resonance after zero and t seconds, provides a rate constant $k_1 = 1.64(11) \times 10^{-5}$ s^{-1} (correlation coefficient R = 0.98) for the first order dissociative reaction step. N7 coordination of 9-Etgua in **15**, which could also be prepared by direct reaction of **1b** with dppz and 9-Etgua in CH_3OH/CH_2Cl_2 solution, is indicated by the downfield shift of *ca.* 0.1 ppm for the neighbouring guanine H8 proton. Although suitable crystals of **15** itself could not be obtained, confirmation of this guanine binding mode is provided by the X-ray structure of the analogous phen derivative $[(\eta^5\text{-}C_5Me_5)Ir(9\text{-Etgua})(phen)](CF_3SO_3)_2$ **16**, whose cation is depicted in Fig. 3. Dihedral angles of 59.4(1) and 29.1(3)° are observed between the plane of the Cp* ligand and respectively those of the phen and 9-Etgua aromatic systems.

Fig. 4 depicts the UV-vis spectra recorded for a buffered 25 μM solution of $[(\eta^5\text{-}C_5Me_5)Ir(H_2metOMe)(dppz)](CF_3SO_3)_3$ **5** at pH 7.2 in the absence and presence of increasing quantities of CT DNA. The observed decrease in absorbance (hypochromicity) at 364 and 382 nm and the bathochromic shifts of these absorption maxima are characteristic for intercalative DNA binding, as has been documented for other polypyridyl metal complexes.[14] An isosbestic point is apparent at 390 nm, in accordance with a simple equilibrium distribution between DNA-bound and free $(\eta^5\text{-}C_5Me_5)Ir^{III}$ complex. All the dppz complexes considered in this work exhibit similar well resolved absorption maxima in the range 350–400 nm, that can be assigned to the π–π* transition of the polypyridyl ligand. Data recorded at 364 nm for the UV-vis titration of **5** with CT DNA were fitted graphically (Fig. 5) using the model of Bard[15] and Thorp[16] to afford least-squares estimates

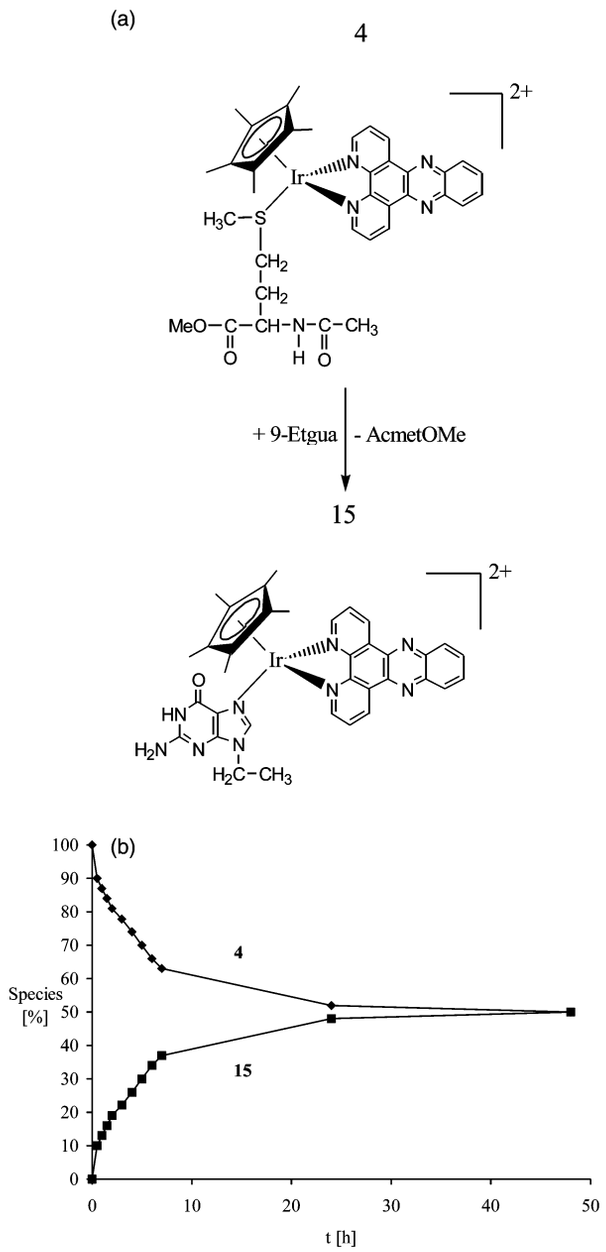

Fig. 2 (a) Substitution of AcmetOMe in **4** by 9-ethylguanine leading to formation of $[(\eta^5\text{-}C_5Me_5)Ir(dppz)(9\text{-}Etgua)]^{2+}$ (**15**); (b) time-dependence of the integral values of the Cp* ^{1}H NMR singlets of **4** and **15**.

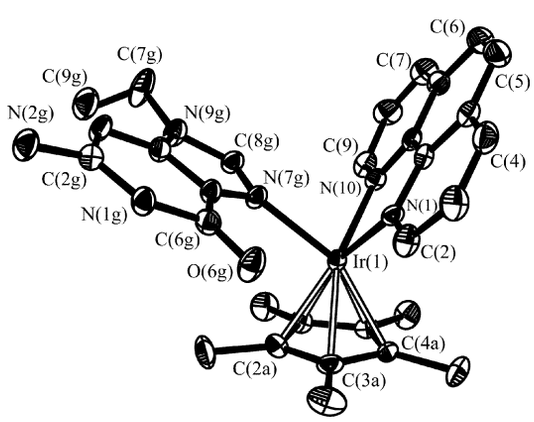

Fig. 3 Molecular structure of the cation of $[(\eta^5\text{-}C_5Me_5)Ir(9\text{-}Etgua)(phen)](CF_3SO_3)_2$ **16** with thermal ellipsoids given at 40% probability. Selected bond lengths (Å): Ir(1)–N(1) 2.120(6), Ir(1)–N(10) 2.106(5), Ir(1)–N(7g) 2.135(6).

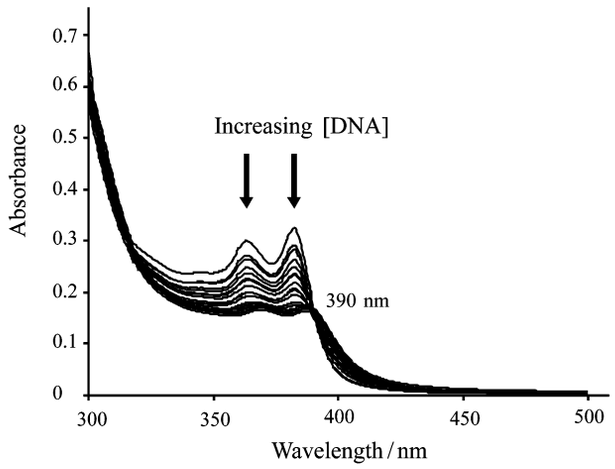

Fig. 4 UV-vis spectra for the titration of $[(\eta^5\text{-}C_5Me_5)Ir(H_2metOMe)(dppz)](CF_3SO_3)_3$ **5** [25 μM] in a 10 mM phosphate buffer (pH 7.2) with CT DNA (0–270 μM).

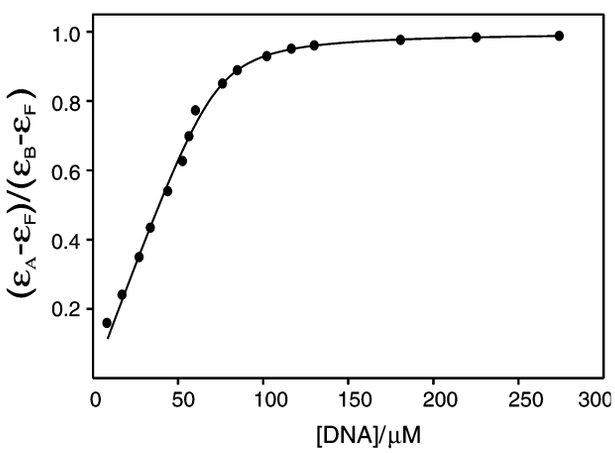

Fig. 5 Best least-squares fit to the model of Bard and Thorp[15,16] for the UV-vis titration data of Fig. 4.

of 2.62(3) × 10^6 M^{-1} for the intrinsic binding constant K_b and 2.02 base pairs of DNA for the average binding site size *s*. Our kinetic study of the substitution of AcmetOMe in $[(\eta^5\text{-}C_5Me_5)Ir(AcmetOMe)(dppz)]^{2+}$ **4** by 9-Etgua suggest that covalent binding of this and other dppz complexes to DNA base nitrogens might possibly compete with intercalation. However, following the initial pronounced hypochromic shift in absorbance on addition of a tenfold excess of CT DNA to a 25 μM solution of **5** at pH 7.2 (see the final trace in Fig. 4), no change in the UV-vis spectrum of the resulting equilibrium mixture was observed over a period of 6 hours. This finding indicates that the intercalative binding mode of such organometallic dppz compounds is indeed strong enough to overwhelmingly subdue any subsequent amino acid/peptide substitution.

Binding constants K_b and site sizes *s* for the dppz complexes **4**–**9** and **13**, **14** are listed in Table 1. The increase in K_b from 8.80(6) × 10^4 M^{-1} through 7.04(5) × 10^5 M^{-1} to 2.62(3) × 10^6 M^{-1} for the series of $(\eta^5\text{-}C_5Me_5)Ir^{III}$ complexes **7** (Aa = AccysOH), **4** (Aa = AcmetOMe) and **5** (Aa = H_2metOMe) clearly reflects a strengthening of the electrostatic interaction with the negatively charged phosphodiester backbone of DNA. Respective net charges of the intercalating complex cations are 1+, 2+ and 3+. An analogous increase in K_b of almost one order of magnitude is also apparent for the trication of $[(\eta^5\text{-}C_5Me_5)Rh(H_2metOMe)(dppz)](CF_3SO_3)_3$ **13** (K_b = 1.26(5) × 10^6 M^{-1}) in comparison to the doubly charged complex cation of $[(\eta^5\text{-}C_5Me_5)Rh(H_2cysOMe)(dppz)](CF_3SO_3)_2$ **14** (K_b = 2.81(7) × 10^5 M^{-1}). A comparable charge effect has recently been reported for a 3+ cobalt–sarcophagine cage complex[17]

Table 1 ΔT_m values of CT DNA, binding constants K_b and site sizes s from UV-vis titration data using eqn. (1). Buffer I (T_m = 70.1 °C) was employed for **4**–**6** and **13**, buffer II (T_m = 72.5 °C) for the remaining metal complexes. The estimated error in ΔT_m is in each case ± 1 °C

Complex	ΔT_m	K_b/M^{-1}	s
$[(\eta^5\text{-Cp*})Ir(AcmetOMe)(dppz)]^{2+}$ **4**	5.8	$7.04(5) \times 10^5$	2.06
$[(\eta^5\text{-Cp*})Ir(H_2metOMe)(dppz)]^{3+}$ **5**	7.8	$2.62(3) \times 10^6$	2.02
$[(\eta^5\text{-Cp*})Ir(HglyglymetOH)(dppz)]^{2+}$ **6**	6.9	$1.16(5) \times 10^6$	1.64
$[(\eta^5\text{-Cp*})Ir(AccysOH)(dppz)]^{+}$ **7**	4.6	$8.80(6) \times 10^4$	1.60
$[(\eta^5\text{-Cp*})Ir(H_2cysOMe)(dppz)]^{2+}$ **8**	7.6	$2.30(4) \times 10^5$	1.53
$[(\eta^5\text{-Cp*})Ir(HglyglycysOH)(dppz)]^{+}$ **9**	6.1	$1.02(4) \times 10^5$	1.81
$[(\eta^5\text{-Cp*})Rh(H_2metOMe)(dppz)]^{3+}$ **13**	8.1	$1.26(5) \times 10^6$	1.53
$[(\eta^5\text{-Cp*})Rh(H_2cysOMe)\ (dppz)]^{2+}$ **14**	6.8	$2.81(7) \times 10^5$	1.69

attached to anthracene, whose K_b value of 1.8×10^6 M^{-1} is also some two orders of magnitude greater than that for the likewise intercalating (9-anthrylmethyl)ammonium(1+) cation.[18] Sartorius and Schneider[12] have demonstrated that the DNA binding of quinoline and naphthalene derivatives can satisfactorily be quantified by adding contributions from the intercalative stacking of their aromatic systems and the electrostatic interactions of ammonium functions in their side chains. Although the H_2metOMe and H_2cysOMe complexes **5**, **8**, **13** and **14** all likewise contain terminal ammonium groups, it is apparent from Table 1, that their DNA binding constants K_b are effectively determined by the total complex charge, *i. e.* $2.62(3) \times 10^6$ and $1.26(5) \times 10^6$ M^{-1} for the 3+ cation of **5** and **13** and $2.30(4) \times 10^5$ and $2.81(7) \times 10^5$ M^{-1} for the 2+ cations of **8** and **14**. Interestingly the K_b value of $1.16(5) \times 10^6$ M^{-1} for the doubly charged cation of $[(\eta^5\text{-}C_5Me_5)Ir(HglyglymetOH)(dppz)]^{2+}$ **6** is comparable to that of **5** and **13**, thereby suggesting that specific ionic or hydrogen bonding interactions could further enhance the intercalative binding of this and other longer oligopeptides.

Thermal denaturation studies for CT DNA revealed changes in the melting point ΔT_m in the range 4.6–8.1 °C (Table 1). The close similarity of the UV-vis spectra obtained after treatment of the $(\eta^5\text{-}C_5Me_5)Ir^{III}$ complexes **4** and **8** with a fourfold excess of either poly(dG-dC)$_2$ or poly(dA-dT)$_2$ indicate the absence of any pronounced site preference for these synthetic polynucleotides. Interestingly, the observed decrease in absorbance at 364 and 382 nm for an equivalent quantity of CT DNA (see Fig. 4) is almost twice as large, thereby suggesting that other competing potential intercalation sites such as GA or GT could be of greater importance. In contrast to the dppz complexes, UV-vis titrations for $[(\eta^5\text{-}C_5Me_5)\ Ir(H_2metOMe)(phen)](CF_3SO_3)_3$ **10** and $[(\eta^5\text{-}C_5Me_5)Ir(H_2cysOMe)(phen)](CF_3SO_3)_2$ **11** provide no evidence for intercalative binding. Fig. 6 depicts the UV-vis spectra recorded for a buffered 25 μM solution of **11** at pH 7.2 in the absence and presence of increasing quantities of CT DNA. The continuous increase in absorbance hyperchromicity at 272 and 369 nm and the associated blue shift of 7 nm are typical for an exclusive electrostatic association between the complex cations and the helix surface. In the addition, the negligible ΔT_m values of 1.7 and 1.4 for the two phen complexes are indicative of an absence of intercalative binding.

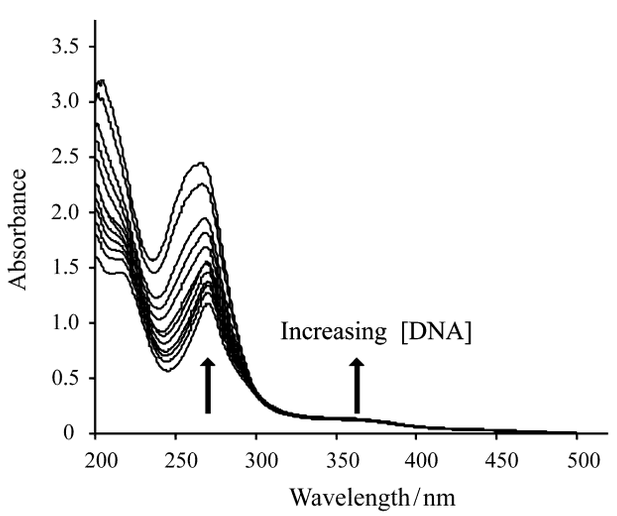

Fig. 6 UV-vis spectra for the titration of $[(\eta^5\text{-}C_5Me_5)Ir(H_2cysOMe)(phen)](CF_3SO_3)_2$ **11** [25 μM] in a 10 mM phosphate buffer (pH 7.2) with CT DNA (0–270 μM).

For a ^{1}H NMR investigation of the possible mode of DNA-binding by complex $[(\eta^5\text{-}C_5Me_5)Ir(H_2metOMe)(dppz)](CF_3SO_3)_3$ **5**, we chose the self-complementary oligonucleotide d(GTCGAC)$_2$. This enables a comparison with Δ-$[Ru(phen)_2dppz]^{2+}$ and Δ-$[Ru(phen)_2dpq]^{2+}$ (dpq = dipyrido[3,2-*d*:2′,3′-*f*]quinoxaline), whose binding to d(GTCGAC)$_2$ has been studied by two-dimensional NOESY.[19–22] As discussed in these previous NMR investigations, the fact that the NOE cross-peak from each purine/pyrimidine H8/H6 proton to its own sugar H2′ proton is significantly larger than that to the H2″ proton (see Fig. 7) allows the conclusion that d(GTCGAC)$_2$ adopts a

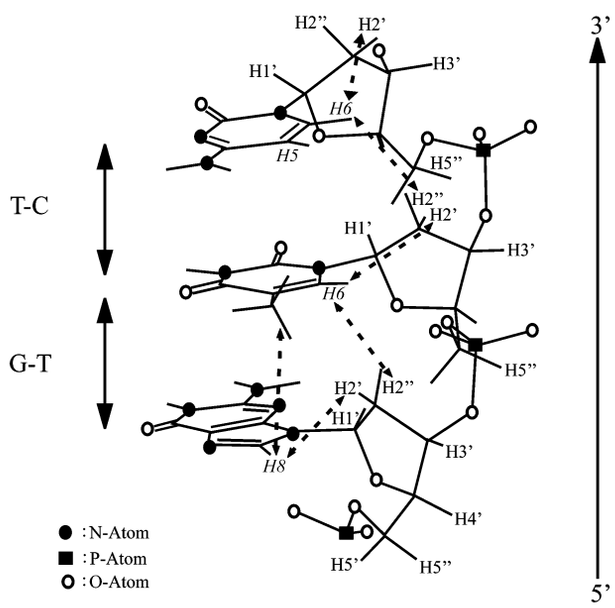

Fig. 7 5′-GTC-3′ segment of the d(GTCGAC)$_2$ hexamer.

B-type confirmation. The relative distances to the H2′ protons are reversed for an A-type duplex. In its NOESY spectrum, an NOE is observed from each base of d(GTCGAC)$_2$ to its own sugar H1′/H2′/H2″ protons as well as to H1′/H2′/H2″ of the flanking 5′-sugar.[19–22]

Addition of **5** to d(GTCGAC)$_2$ at a 1 : 1 molar ratio induces marked upfield shifts and broadening of the dppz proton resonances (Fig. 8), both of which phenomena are indicative of intercalative DNA binding by the polypyridyl ligand. The larger shifts of −0.37, −0.28 and −0.21 ppm for the respective (4,7), (16, 19) and (17, 18) resonances (Scheme 2) also suggest that these protons must be sited closer to the centre of the base

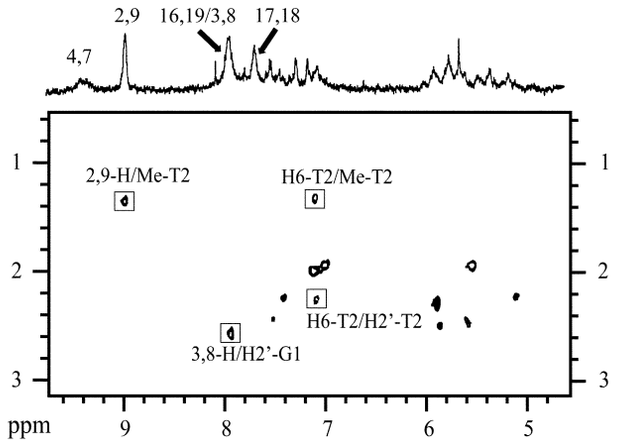

Fig. 8 2D-NOESY spectrum of the aromatic-sugar H2′ region of the $[(\eta^5\text{-}C_5Me_5)Ir(H_2metOMe)(dppz)](CF_3SO_3)_3$–d(GTCGAC)$_2$ reaction mixture in a 10 mM phosphate buffer [pH 7.2] at 283 K.

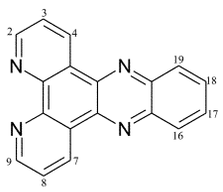

Scheme 2 Numbering scheme for the dppz ligand.

stack, where ring current effects will be most substantial, than their (3,8) and (2,9) counterparts (−0.15 and −0.02 ppm). Further evidence for the stability of this intercalative binding with respect to possible covalent Ir–N(base) binding is provided by the observation that the resonance position of the Cp* methyl protons remains unchanged at 1.82 ppm, as for the free complex **5**, over a period of 24 hours. In the 300 ms NOESY spectrum of the 1 : 1 **5**–d(GTCGAC)$_2$ complex depicted in Fig. 8 new NOE cross peaks are apparent for the dppz (2,9) and (3,8) protons with respectively T_2-CH_3 and a purine sugar H2′. The presence of the former NOE is consistent with a sequence-selective intercalation at T_2C_3/A_5G_4 or G_1T_2/C_6A_5 in the major groove. An additional dppz–base NOE cross peak for the (2,9) protons of the polypyridyl ligand at 9.05/8.02 ppm could be caused by intermolecular proximity to a guanine H8. This suggests that, as for Δ-$[Ru(phen)_2(dppz)]^{2+}$ bound to d(GTCGAC)$_2$ intercalation of the dppz ligand[19,20] may preferentially take place at G_1T_2/C_6A_5, albeit in this case between G_1 and T_2 rather than C_6 and A_5. In accordance with this assumption is the absence of an NOE cross peak between T_2-H6 and the sugar proton G_1-H2″ (see Fig. 7). The ^{1}H NMR spectrum taken for a 1:1 $[(\eta^5\text{-}C_5Me_5)Ir(H_2cysOMe)(phen)](CF_3SO_3)_2$–d(GTCGAC)$_2$ reaction mixture confirms the UV-vis titration finding (Fig. 6) that complex **11** does not intercalate into DNA. The phen protons remain unshifted and the characteristic signal broadening for this binding mode is not observed.

DNA binding and cleavage assays

Intercalation of metal complexes into plasmid DNA leads to local unwinding of the double helix and a concomitant decrease in mobility, that can be detected by gel electrophoresis on an agarose gel. Lanes 1–7 of Fig. 9a show the effect of steadily increasing quantities (10–70 μM) of $[(\eta^5\text{-}C_5Me_5)Ir(H_2metOMe)(dppz)](CF_3SO_3)_3$ **5** on the plasmid *pBluescript II KS+*, in comparison to the untreated plasmid (lane 8). The observed decrease in mobility could result from both local unwinding of the double helix and reduction in the overall negative charge of DNA, caused by the sugar-phosphate backbone. If the latter effect were indeed to be of major significance in controlling the electrophoretic migration of the treated

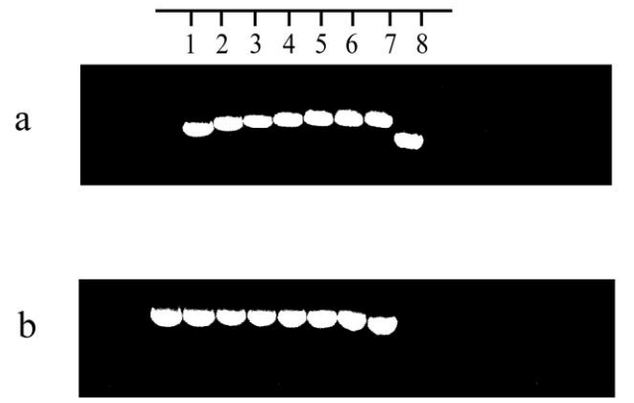

Fig. 9 Photographic positive of a 0.8% agarose gel showing the interaction of $[(\eta^5\text{-}C_5Me_5)Ir(H_2metOMe)(dppz)](CF_3SO_3)_3$ **5** and $[(\eta^5\text{-}C_5Me_5)Ir(H_2cysOMe)(bpy)](CF_3SO_3)_2$ **17** with plasmid *pBluescript II KS+*: (a) lanes 1–7 for 10, 20, 30, 40, 50, 60, 70 μM **5** + plasmid (62 μM); (b) lanes 1–7 for 10, 20, 30, 40, 50, 60, 70 μM **17** + plasmid (62 μM). All samples were incubated for 60 min at 37 °C. Outer lanes 8 show the untreated plasmid.

plasmid DNA through the agarose gel, then a similar retardation should be observed for the nonintercalating complex $[(\eta^5\text{-}C_5Me_5)Ir(H_2cysOMe)(bpy)](CF_3SO_3)_2$ **17**, prepared for this purpose by method A (see below). Fig. 9b indicates that this is not the case and, thereby, demonstrates that intercalation of the strongly binding complex **5** (K_b = 2.62(3) × 10^6 M^{-1}) must primarily be responsible for the reduced mobility of the treated plasmid DNA.

Photochemical cleavage of the supercoiled *pBluescript II KS+* was examined for complexes **4**–**6**. Following incubation of an equimolar complex/plasmid reaction mixture at 37 °C for 60 min, samples were irradiated for 30–180 s with a high pressure Hg lamp. It is apparent from the photographs presented in Fig. 10, that the three metal complexes yield different quantities of

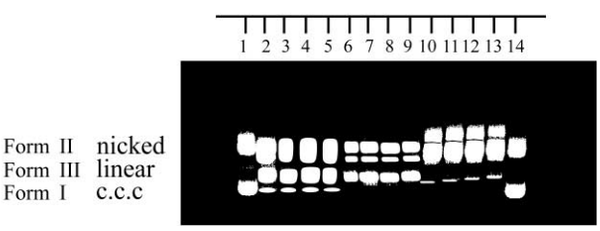

Fig. 10 Photographic positive of a 1% agarose gel showing photolytic cleavage of plasmid *pBluescript II KS+* with a high pressure 500 W Hg lamp: lane 1 for untreated plasmid without irradiation; lanes 2–5, 62 μM plasmid + 60 μM **4** for 30, 60, 120 and 180 s irradiation; lanes 6–9 and 10–13 for similar experiments with respectively **6** and **5**; lane 14 for untreated plasmid after 180 s irradiation.

DNA cleavage products, as detected by changes in the electrophoretic mobility. If scission occurs in one strand (nicking), then the supercoiled plasmids (Form I, covalently-closed DNA) will relax to generate a slower-moving open circular form (Form II, nicked circular DNA). When both strands are cleaved, a linear form (Form III) with an intermediate mobility will result. The relatively short irradiation periods lead to transformation of the supercoiled plasmid DNA into both its nicked and linear forms. Cleavage of both strands to generate Form III is particularly pronounced in the presence of complexes **5** (lanes 2–5) and **6** (lanes 10–13). As photolysis of untreated plasmid DNA (lane 14) does not lead to such a new scission band, it is clear that double cleavage must require the close proximity of the $(\eta^5\text{-}C_5Me_5)Ir^{III}$ intercalators to DNA.

Our present findings indicate that the strength of DNA binding for cationic complexes of the type $[(\eta^5\text{-}C_5Me_5)Ir(Aa)(dppz)]^{n+}$ (n = 1–3) is clearly dependent on the magnitude of the positive charge n. As demonstrated for HglyglymetOH

and HglyglycysOH, S-bound peptides can be employed as bioligands instead of the parent amino acids and their derivatives. This suggests, in analogy[13] to $[Rh(phi)_2(phen')]^{3+}$, that DNA site specificity might be achieved for such bioorganometallic complexes by introduction of longer met- or cys-containing oligopeptides containing chosen sequences of amino acid residues with side-chain functional groups.

Experimental

Materials

Amino acids (AcmetOMe, H_2metOMe, AccysOH and H_2cysOMe) and peptides (HglyglymetOH and HglyglycysOH with HglyOH = glycine) were purchased from Bachem (Heidelberg) and used as received. Metal salts $IrCl_3 \cdot xH_2O$ and $RhCl_3 \cdot xH_2O$ were obtained from ChemPur. The starting compounds $[(\eta^5\text{-}C_5Me_5)Ir(Me_2CO)_3](CF_3SO_3)_2$ **1b** and $[(\eta^5\text{-}C_5Me_5)Rh(Me_2CO)_3](CF_3SO_3)_2$ **2b** were prepared from respectively $[(\eta^5\text{-}C_5Me_5)IrCl_2]_2$ **1a** or $[(\eta^5\text{-}C_5Me_5)RhCl_2]_2$ **2a** by addition of an equivalent amount of $Ag(CF_3SO_3)$ and filtration of the precipitated AgCl in acetone.[23,24] Dipyrido[3, 2-*a*:2′,3′-*c*]phenazine (dppz) was synthesized according to a literature procedure.[25,26] (1,10)-Phenanthroline (phen) was purchased from Aldrich and used as received, as was calf thymus DNA (CT DNA) from Sigma. The plasmid *pBluescript II KS+* (supercoiled as linearized) was a gift from the Department of Biochemistry of the Ruhr University of Bochum. Poly- and hexa-nucleotides {poly(dA-dT)$_2$, poly(dG-dC)$_2$ and d(GTCGAC)$_2$} were synthesized on an Pharmacia Gene Assembler Special synthesizer. High-strength, analytical grade agarose was obtained from MBI Fermentar. All other reagents and solvents were analytical reagents grade, and were used as received.

Mass spectral and NMR measurements

The FAB mass spectra were recorded on a Fisons VG Autospec instrument employing 3-nitrobenzyl alcohol as the matrix, IR spectra as KBr discs on a Perkin-Elmer 1760 spectrometer. Microanalyses (C, H, N and S) were performed using a VarioEL elemental analyser (Elementar Analysensysteme GmbH). ^{1}H and ^{13}C NMR spectra were recorded on a Bruker DRX 400 spectrometer using 5 mm tubes. Chemical shifts are reported as δ values relative to the signal of the deuterated solvent. 2D-ROESY and -NOESY spectra were acquired on a Bruker DRX 600 spectrometer at 283 K with a mixing time of 300 ms using 2.5 mm tubes and referenced to sodium 3-(trimethylsilyl)tetradeuteriopropionate (TSP). UV-vis spectra were taken on a Perkin-Elmer Lambda 15 spectrometer.

DNA binding studies

The thermal denaturation temperature of complex/DNA mixtures (1 : 10) was determined either in buffer I (10 mM phosphate buffer, 20 mM NaCl, pH 7.2) or in buffer II (10 mM phosphate buffer, pH 7.2). Melting curves were recorded at 260 nm on a Lambda 15 Perkin-Elmer spectrophotometer connected to a temperature controller (HAAKE FS thermostat). A ramp rate of 0.25 °C min^{-1} was used over the range 25–90 °C. The melting temperatures of the native and modified DNA were calculated by determining the midpoints of the melting curves from the first-order derivatives. Binding constants (K_b) and site sizes (s) were determined by UV absorption titrations at room temperature for which concentrations of nucleic acids were determined using the following molar absorption coefficients at the given wavelengths: $\varepsilon_{254\ nm}$ = 8400 M^{-1} cm^{-1} for poly(dG-dC)$_2$ and $\varepsilon_{260\ nm}$ = 6600 M^{-1} cm^{-1} for poly(dA-dT)$_2$, d(GTCGAC)$_2$ and CT DNA.[27] After sonication, the solutions of CT DNA in the appropriate buffer gave a ratio of UV absorbance at A_{260}/A_{280} of *ca.* 1.90, indicating that the DNA was sufficiently free of protein.[28] Fixed quantities of metal complexes were titrated with DNA over a range of DNA concentrations from 0 to 300 μM. All UV spectra were measured after equilibration (no further change in the monitoring absorbance). Titration curves were constructed from the fractional change in the absorption intensity as a function of DNA concentration according to the model of Thorp and Bard.[15,16] Eqn. (1) was used to provide a least-squares fit to the absorption data by refining the binding constants (K_b) and site sizes (s):

$$(\varepsilon_a - \varepsilon_f)/(\varepsilon_b - \varepsilon_f) = (b - \{b^2 - 2K_b^2 c_t[\mathrm{DNA}]/s\}^{1/2})/2K_b c_t \quad (1)$$
$$b = 1 + K_b c_t + K_b[\mathrm{DNA}]/2s$$

where ε_a is the absorption coefficient observed at a given DNA concentration, ε_f is the absorption coefficient of the complex in the absence of DNA, ε_b is the absorption coefficient of the complex when fully bound to DNA (no absorption change by further addition of DNA), K_b is the equilibrium binding constant in M^{-1}, c_t is the total metal complex concentration, [DNA] is the DNA concentration in M (nucleotide), and s is the binding site size.

Gel electrophoresis

Horizontal gel electrophoresis studies employed 0.8 or 1.0% (wt./vol.) agarose in a TBE buffer (90 mM Tris base, 90 mM boric acid, 2.2 mM H_4EDTA, pH 8.3). Electrophoresis proceeded at 110 V for 2.5 h with recirculation of the buffer. Gels were then stained in 0.5 μg m^{-1}l ethidium bromide for 30 min and photographed with UV illumination as Polaroid prints. Photolyses of the reaction mixtures (plasmid/metal complex, 25 μl, 37 °C, 1 h) were performed with a high pressure 500 W Hg lamp (Ushio) using a 295 nm "Cut-off" filter. The samples in microcentrifuge tubes (Eppendorf) were held vertically 15 cm from the lamp for the times designated.

Syntheses

All reactions were carried out under argon using standard Schlenk techniques. Complexes were generally prepared by one of the three following methods.

Method A. 0.13 mmol of the starting compound (**1b** or **2b**) was dissolved in 10 ml CH_3OH/CH_2Cl_2 (1 : 1) and stirred for 2 h at reflux after adding 0.13 mmol of the corresponding polypyridyl ligand (dppz or phen). An equivalent amount of amino acid (AcmetOMe, AccysOH) was then added and the solution stirred for the time and temperature designated. In the case of the hydrochlorides HmetOMe·HCl or HcysOMe·HCl solutions of these (0.13 mmol) in 5 ml methanol were stirred with 0.13 mmol $Ag(CF_3SO_3)$ for 30 min and the precipitated AgCl removed by centrifugation at 5 °C prior to employment. After reduction of the solvent volume to *ca.* 4 ml, addition of diethyl ether led to the precipitation of the desired product which was washed three times with Et_2O and dried at 50 °C in vacuum.

Method B. 0.13 mmol of the starting material **1b** was dissolved in 10 ml CH_3OH/CH_2Cl_2 (1 : 1) and stirred for 2 h at reflux after addition of 0.13 mmol of the respective ligand (dppz or phen). After cooling the resulting solution, addition of 2 ml CF_3COOH and 0.13 mmol peptide (HglyglymetOH or HglyglycysOH) yielded a suspension which was stirred for the time and temperature designated. The solution was then reduced in volume to *ca.* 3 ml. After precipitation with diethyl ether the resulting solid was washed three times with Et_2O and dried for several hours at 50 °C in vacuum.

Method C. A solution containing 0.13 mmol $[(\eta^5\text{-}C_5Me_5)IrCl_2]_2$ **1a** or $[(\eta^5\text{-}C_5Me_5)RhCl_2]_2$ **2a** in 10 ml acetone was stirred with 0.065 mmol $Ag(CF_3SO_3)$ for 30 min at room temperature.

The precipitated AgCl was centrifuged at 5 °C and the solution dried in vacuum. After addition of 10 ml CH_3OH/CH_2Cl_2 and 0.13 mmol dppz the resulting solution was stirred for 2 h at 75 °C and then removed in vacuum. The remaining solid was dissolved in 3 ml methanol and the product precipitated with diethyl ether and dried for several hours in vacuum.

[(η^5-C_5Me_5)Ir(Cl)(dppz)](CF_3SO_3) 3. Method C, 2 h, 75 °C. Yield 94.0 mg, 91% (Found: C, 43.6; H, 3.1; N, 7.1; S, 4.0. Calc. for $C_{29}H_{25}ClF_3IrN_4O_3S$: C, 43.9; H, 3.2; N, 7.1; S, 4.0%). FAB mass spectrum: *m/z* 609.9 (47, $[M - Cl - CF_3SO_3]^+$) and 644.8 (100%, $[M - CF_3SO_3]^+$). ^{1}H NMR (DMSO): δ 1.74 (s, 15H, Cp*), 8.17 (m, 2H), 8.36 (m, 2H), 8.48 (m, 2H), 9.46 (dd, 2H), 9.75 (dd, 2H). ^{13}C NMR (DMSO): δ 8.4 (Cp*), 89.6 (Cp*), 129.1, 129.7, 130.0, 132.9, 136.0, 139.7, 142.2, 149.3, 153.7. UV-VIS (DMSO): λ_{max}/nm (ε_{max}/$M^{-1}cm^{-1}$), 279 (3.6×10^4), 362 (0.8×10^4) and 382 (0.8×10^4).

[(η^5-C_5Me_5)Ir(AcmetOMe)(dppz)](CF_3SO_3)$_2$ 4. Method A, 18 h, 60 °C. Yield 120.1 mg, 83% (Found: C, 40.6; H, 4.0; N, 5.9; S, 8.7. Calc. for $C_{38}H_{40}F_6IrN_5O_9S_3$: C, 41.0; H, 3.6; N, 6.3; S, 8.6%). FAB mass spectrum: *m/z* 610.1 (100, [(η^5-Cp*)-Ir(dppz)]$^+$), 759.0 (77, [(η^5-Cp*)Ir(dppz) + $CF_3SO_3]^+$) and 964.1 (71%, $[M - CF_3SO_3]^+$). ^{1}H NMR (CD_3OD): δ 1.88 (s, 3H, δ-CH_3), 1.89 (s, 15H, Cp*), 1.91 (s, 3H, CH_3 Ac), 1.96–2.05 (mm, 4H, β- + γ-CH_2), 3.68 (s, 3H, CH_3 OMe), 4.39 (m, 1H, α-CH), 8.21 (m, 2H), 8.49 (m, 2H), 8.59 (m, 2H), 9.41 (dd, 2H), 10.11 (dd, 2H). ^{13}C NMR (CD_3OD): δ 8.7 (Cp*), 17.2 (δ-CH_3), 22.8 (CH_3 Ac), 30.3 (β-CH_2), 34.0 (γ-CH_2), 52.1 (α-CH), 53.4 (CH_3 OMe), 97.4 (Cp*), 130.7, 131.3, 133.8, 134.3, 139.4, 141.1, 144.7, 151.8, 155.8, 172.8, 173.5. $\tilde{\nu}_{max}$/cm^{-1} 3316 (ν NH), 1742, 1671 (ν CO), 1540 (δ NH). UV-VIS (H_2O): λ_{max}/nm (ε_{max}/$M^{-1}cm^{-1}$), 280 (4.6×10^4), 364 (1.0×10^4) and 382 (1.1×10^4).

[(η^5-C_5Me_5)Ir(H_2metOMe)(dppz)](CF_3SO_3)$_3$ 5. Method A, 18 h, 60 °C. Yield 127.0 mg, 80% (Found: C, 36.0; H, 3.3; N, 5.4; S, 10.7. Calc. for $C_{37}H_{39}F_9IrN_5O_{11}S_4$: C, 36.3; H, 3.2; N, 5.7; S, 10.5%). FAB mass spectrum: *m/z* 610.1 (100, [(η^5-Cp*)-Ir(dppz)]$^+$), 759.0 (84, [(η^5-Cp*)Ir(dppz) + $CF_3SO_3]^+$), 922.1 (68, $[M - 2CF_3SO_3]^+$) and 1072.0 (66%, $[M - CF_3SO_3]^+$). ^{1}H NMR (CD_3OD): δ 1.88 (s, 3H, δ-CH_3), 1.89 (s, 15H, Cp*), 1.96–2.09 (mm, 4H, β- + γ-CH_2), 3.79 (s, 3H, CH_3 OMe), 3.92 (dd, 1H, α-CH), 8.21 (m, 2H), 8.50 (m, 2H), 8.59 (m, 2H), 9.45 (dd, 2H), 10.11 (dd, 2H). ^{13}C NMR (CD_3OD): δ 8.7 (Cp*), 16.8 (δ-CH_3), 29.0 (β-CH_2), 33.1 (γ-CH_2), 52.4 (α-CH), 54.4 (CH_3 OMe), 97.5 (Cp*), 130.8, 131.2, 133.9, 134.2, 139.5, 141.1, 144.7, 151.8, 155.9, 169.6. $\tilde{\nu}_{max}$/cm^{-1} 3495 (ν NH), 1751 (ν CO), 1625, 1499 (δ NH). UV-VIS (H_2O): λ_{max}/nm (ε_{max}/$M^{-1}cm^{-1}$), 206 (4.3×10^4), 281 (6.0×10^4), 363 (1.3×10^4) and 382 (1.3×10^4).

[(η^5-C_5Me_5)Ir(HglyglymetOH)(dppz)](CF_3SO_3)$_2$ 6. Method B, 24 h, 50 °C. Yield 123.3 mg, 81% (Found: C, 38.1; H, 3.3; N, 7.1; S, 6.8. Calc. for $C_{39}H_{42}F_6IrN_7O_{10}S_3 \cdot CF_3CO_2H$: C, 38.3; H, 3.3; N, 7.6; S, 7.5%). FAB mass spectrum: *m/z* 610.2 (100, [(η^5-Cp*)Ir(dppz)]$^+$), 872.3 (63, $[M - 2CF_3SO_3]^+$) and 1022.4 (59%, $[M - CF_3SO_3]^+$). ^{1}H NMR (CD_3OD): δ 1.85 (s, 3H, δ-CH_3), 1.89 (s, 15H, Cp*), 2.12 (br, 4H, β- + γ-CH_2), 3.68 (s, 2H, α_{gly}-CH_2), 3.81 (s, 2H, α_{gly}-CH_2), 4.08 (dd, 1H, α-CH), 8.22 (dd, 2H), 8.53 (m, 2H), 8.59 (dd, 2H), 9.43 (dd, 2H), 10.11 (dd, 2H). ^{13}C NMR (CD_3OD): δ 8.7 (Cp*), 17.2 (δ-CH_3), 30.8 (β-CH_2), 34.8 (γ-CH_2), 41.9 (α-CH), 44.0, 54.7 (α_{gly}-CH_2), 97.3 (Cp*), 121.3 (q, $CF_3SO_3^-$), 130.8, 131.2, 133.7, 134.2, 139.3, 141.2, 144.7, 151.7, 155.8, 168.5, 170.9, 176.2. $\tilde{\nu}_{max}$/cm^{-1} 3464 (ν NH), 1747, 1677 (ν CO), 1546 (δ NH). UV-VIS (H_2O): λ_{max}/nm (ε_{max}/$M^{-1}cm^{-1}$), 282 (4.6×10^4), 364 (1.0×10^4) and 382 (1.1×10^4).

[(η^5-C_5Me_5)Ir(AccysOH)(dppz)](CF_3SO_3) 7. Method A, 6 h, 45 °C. Yield 101.8 mg, 85% (Found: C, 43.9; H, 3.9; N, 7.8; S, 6.5. Calc. for $C_{34}H_{33}F_3IrN_5O_6S_2$: C, 44.3; H, 3.6; N, 7.6; S, 7.0%). FAB mass spectrum: *m/z* 610.1 (83, [(η^5-Cp*)Ir(dppz)]$^+$) and 772.1 (100%, $[M - CF_3SO_3]^+$). ^{1}H NMR (CD_3OD): δ 1.74 (s, 3H, CH_3 Ac), 1.86 (s, 15H, Cp*), 1.92, 2.04 (2dd, 2H, β-CH_2), 3.61 (dd, 1H, α-CH), 8.16 (m, 2H), 8.32 (m, 2H), 8.50 (m, 2H), 9.29 (dd,), 9.85 (dd, 2H). ^{13}C NMR (CD_3OD): δ 8.6 (Cp*), 22.4 (CH_3 Ac), 29.4 (β-CH_2), 52.7 (α-CH), 93.2 (Cp*), 129.8, 131.1, 132.6, 134.0, 137.1, 141.1, 144.4, 151.4, 154.6, 172.9. $\tilde{\nu}_{max}$/cm^{-1} 3435 (ν NH), 1743 (ν CO), 1646, 1496 (δ NH). UV-VIS (H_2O): λ_{max}/nm (ε_{max}/$M^{-1}cm^{-1}$), 208 (3.0×10^4), 281 (3.6×10^4), 363 (0.8×10^4) and 381 (0.7×10^4).

[(η^5-C_5Me_5)Ir(H_2cysOMe)(dppz)](CF_3SO_3)$_2$ 8. Method A, 6 h, 45 °C. Yield 119.3 mg, 88% (Found: C, 38.7; H, 3.4; N, 6.3; S, 8.7. Calc. for $C_{34}H_{34}F_6IrN_5O_8S_3$: C, 39.1; H, 3.3; N, 6.7; S, 9.2%). FAB mass spectrum: *m/z* 610.0 (97, [(η^5-Cp*)Ir(dppz)]$^+$), 744.0 (100, $[M - 2CF_3SO_3]^+$) and 894.0 (81%, $[M - CF_3SO_3]^+$). ^{1}H NMR (CD_3OD): δ 1.88 (s, 15H, Cp*), 2.05, 2.18 (2dd, 2H, β-CH_2), 3.45 (sh, 1H, α-CH), 3.47 (s, 3H, CH_3 OMe), 8.19 (dd, 2H), 8.36 (dd, 2H), 8.54 (dd, 2H), 9.32 (d, 2H), 9.93 (dd, 2H). ^{13}C NMR (CD_3OD): δ 8.7 (Cp*), 27.3 (β-CH_2), 53.7 (α-CH), 56.3 (CH_3 OMe), 93.4 (Cp*), 129.9, 131.2, 132.7, 134.1, 137.3, 141.2, 144.6, 151.2, 154.7, 169.4. $\tilde{\nu}_{max}$/cm^{-1} 3480 (ν NH), 1747 (ν CO), 1634, 1495 (δ NH). UV-VIS (H_2O): λ_{max}/nm (ε_{max}/$M^{-1}cm^{-1}$), 280 (5.2×10^4), 362 (1.1×10^4) and 380 (1.0×10^4).

[(η^5-C_5Me_5)Ir(HglyglycysOH)(dppz)](CF_3SO_3) 9. Method B, 24 h, 50 °C. Yield 95.6 mg, 74% (Found: C, 43.0; H, 3.9; N, 9.4; S, 6.7. Calc. for $C_{36}H_{38}F_3IrN_7O_7S_2$: C, 43.5; H, 3.9; N, 9.8; S, 6.4%). FAB mass spectrum: *m/z* 610.1 (100, [(η^5-Cp*)-Ir(dppz)]$^+$), 759.1 (82, [(η^5-Cp*)Ir(dppz) + $CF_3SO_3]^+$) and 844.1 (96%, $[M - CF_3SO_3]^+$). ^{1}H NMR (CD_3OD): δ 1.87 (s, 15H, Cp*), 1.93, 2.06 (2dd, 2H, β-CH_2), 3.67 (sh, 1H, α-CH), 3.69 (s, 2H, α_{gly}-CH_2), 3.79 (s, 2H, α_{gly}-CH_2), 8.17 (m, 2H), 8.32 (dd, 2H), 8.52 (m, 2H), 9.30 (dd, 2H), 9.87 (dd, 2H). ^{13}C NMR (CD_3OD): δ 8.7 (Cp*), 29.2 (β-CH_2), 41.7, 43.0 (α_{gly}-CH_2), 56.7 (α-CH), 93.1 (Cp*), 129.8, 131.2, 132.8, 133.9, 137.1, 138.5, 141.2, 144.5, 154.6, 167.9, 171.5, 173.6. $\tilde{\nu}_{max}$/cm^{-1} 3323 (ν NH), 1674 (ν CO), 1541 (δ NH). UV-VIS (H_2O): λ_{max}/nm (ε_{max}/$M^{-1}cm^{-1}$), 280 (4.6×10^4), 362 (0.9×10^4) and 382 (0.8×10^4).

[(η^5-C_5Me_5)Ir(H_2metOMe)(phen)](CF_3SO_3)$_3$ 10. Method A, 18 h, 60 °C. Yield 120.8 mg, 83% (Found: C, 32.7; H, 3.2; N, 3.7; S, 11.2. Calc. for $C_{31}H_{37}F_9IrN_3O_9S_4$: C, 33.3; H, 3.3; N, 3.8; S, 11.4%). FAB mass spectrum: *m/z* 508.1 (100, [(η^5-Cp*)-Ir(phen)]$^+$), 657.2 (93, [(η^5-Cp*)Ir(phen) + $CF_3SO_3]^+$), 820.1 (91, $[M - 2CF_3SO_3]^+$) and 970.0 (90%, $[M - CF_3SO_3]^+$). ^{1}H NMR (CD_3OD): δ 1.71 (s, 3H, δ-CH_3), 1.86 (s, 15H, Cp*), 1.96 (mm, 4H, β- u. γ-CH_2), 3.78 (s, 3H, CH_3 OMe), 3.97 (m, 1H, α-CH), 8.37 (m, 2H), 8.43 (s, 2H), 9.09 (dd, 2H), 9.41 (m, 2H). ^{13}C NMR (CD_3OD): δ 8.7 (Cp*), 16.6 (δ-CH_3), 29.0 (β-CH_2), 33.0 (γ-CH_2), 52.3 (α-CH), 54.3 (CH_3 OMe), 97.2 (Cp*), 129.6, 130.4, 133.8, 142.7, 148.8, 155.3, 169.6. $\tilde{\nu}_{max}$/cm^{-1} 3480 (ν NH), 1751 (ν CO), 1636, 1520 (δ NH). UV-VIS (H_2O): λ_{max}/nm (ε_{max}/$M^{-1}cm^{-1}$), 220 (3.0×10^4), 276 (3.4×10^4), 357 (1.5×10^4).

[(η^5- C_5Me_5)Ir(H_2cysOMe)(phen)](CF_3SO_3)$_2$ 11. Method A, 6 h, 45 °C. Yield 100.3 mg, 82% (Found: C, 35.3; H, 3.3; N, 4.2; S, 10.2. Calc. for $C_{28}H_{32}F_6IrN_3O_8S_3$: C, 35.7; H, 3.4; N, 4.5; S, 10.2%). FAB mass spectrum: *m/z* 508.1 (100, [(η^5-Cp*)-Ir(phen)]$^+$), 642.1 (88, $[M - 2CF_3SO_3]^+$) and 792.0 (54%, $[M - CF_3SO_3]^+$). ^{1}H NMR (CD_3OD): δ 1.84 (s, 15H, Cp*), 1.92–2.06 (m, 2H, β-CH_2), 3.38 (sh, 1H, α-CH), 3.50 (s, 3H, CH_3 OMe), 8.22 (m, 2H), 8.34 (s, 2H), 8.90 (m, 2H), 9.26 (m, 2H). ^{13}C NMR (CD_3OD): δ 8.7 (Cp*), 27.1 (β-CH_2), 53.7 (CH_3 OMe), 56.3 (α-CH), 93.3 (Cp*), 122.1 (q, $CF_3SO_3^-$), 128.7, 129.8, 133.2, 140.5, 148.5, 153.6, 169.4. $\tilde{\nu}_{max}$/cm^{-1} 3466 (ν NH), 1752 (ν CO), 1606, 1516 (δ NH). UV-VIS (H_2O): λ_{max}/nm (ε_{max}/$M^{-1}cm^{-1}$), 217 (3.0×10^4), 272 (2.6×10^4), 369 (0.2×10^4).

[(η⁵-C_5Me_5)Rh(Cl)(dppz)](CF_3SO_3) 12. Method C, 2 h, 75 °C. Yield 81.6 mg, 89% (Found: C, 48.8; H, 3.5; N, 7.8; S, 4.5. Calc. for $C_{29}H_{25}ClF_3N_4O_3RhS$: C, 49.4; H, 3.6; N, 7.9; S, 4.5%). FAB mass spectrum: *m/z* 519.1 (51, $[M - Cl - CF_3SO_3]^+$) and 555.1 (100%, $[M - CF_3SO_3]^+$). ^{1}H NMR (DMSO): δ 1.75 (s, 15H, Cp*), 8.12 (dd, 2H), 8.38 (m, 2H), 8.42 (m, 2H), 9.47 (d, 2H), 9.74 (d, 2H). ^{13}C NMR (DMSO): δ 8.7 (Cp*), 97.4 (Cp*), 128.6, 129.6, 130.1, 132.7, 135.9, 139.6, 142.1, 147.8, 153.7. UV-VIS (DMSO): λ_{max}/nm (ε_{max}/$M^{-1}cm^{-1}$), 256 (5.8×10^4), 362 (1.0×10^4), 380 (1.0×10^4).

[(η⁵-C_5Me_5)Rh(H_2metOMe)(dppz)](CF_3SO_3)$_3$ 13. Method A, 18 h, 60 °C. Yield 126.6 mg, 86% (Found: C, 38.7; H, 3.4; N, 6.1; S, 10.0. Calc. for $C_{37}H_{39}F_9N_5O_{11}RhS_4$: C, 39.3; H, 3.5; N, 6.2; S, 11.3%). FAB mass spectrum: *m/z* 520.1 (100, [(η⁵-Cp*)-Rh(dppz)]$^+$), 833.3 (1, $[M - 2CF_3SO_3]^+$) and 982.1 (1%, $[M - CF_3SO_3]^+$). ^{1}H NMR (CD_3OD): δ 1.86 (s, 3H, δ-CH_3), 1.90 (s, 15H, Cp*), 2.14 (mm, 4H, β- u. γ-CH_2), 3.78 (s, 3H, CH_3 OMe), 4.01 (dd, 1H, α-CH), 8.19 (m, 2H), 8.52 (m, 2H), 8.57 (dd, 2H), 9.43 (d, 2H), 10.13 (d, 2H). ^{13}C NMR (CD_3OD): δ 9.2 (Cp*), 17.2 (δ-CH_3), 29.3 (β-CH_2), 33.3 (γ-CH_2), 52.3 (α-CH), 54.3 (CH_3 OMe), 104.3 (Cp*), 123.5 (q, $CF_3SO_3^-$), 130.6, 131.2, 133.5, 134.0, 139.5, 141.1, 144.7, 150.1, 155.8, 169.6. $\tilde{\nu}_{max}$/cm^{-1} 3520 (ν NH), 1745 (ν CO), 1627, 1506 (δ NH). UV-VIS (H_2O): λ_{max}/nm (ε_{max}/$M^{-1}cm^{-1}$), 257 (8.6×10^4), 361 (1.4×10^4), 379 (1.5×10^4).

[(η⁵-C_5Me_5)Rh(H_2cysOMe)(dppz)](CF_3SO_3)$_2$ 14. Method A, 6 h, 45 °C. Yield 99.2 mg, 80% (Found: C, 42.5; H, 3.4; N, 7.0; S, 9.7. Calc. for $C_{34}H_{34}F_6N_5O_8RhS_3$: C, 42.8; H, 3.6; N, 7.3; S, 10.1%). FAB mass spectrum: *m/z* 520.1 (100, [(η⁵-Cp*)-Rh(dppz)]$^+$), 654.2 (79, $[M - 2CF_3SO_3]^+$) and 804.1 (76%, $[M - CF_3SO_3]^+$). ^{1}H NMR (CD_3OD): δ 1.85 (s, 15H, Cp*), 1.95 (m, 2H, β-CH_2), 3.23 (br, 1H, α-CH), 3.42 (s, 3H, CH_3 OMe), 8.17 (dd, 2H), 8.41 (dd, 2H), 8.53 (dd, 2H), 9.33 (dd, 2H), 9.98 (dd, 2H). ^{13}C NMR (CD_3OD): δ 9.0 (Cp*), 28.6 (β-CH_2), 53.7 (CH_3 OMe) 56.3 (α-CH), 100.3 (Cp*), 120.5 (q, $CF_3SO_3^-$), 129.7, 130.3, 132.3, 134.0, 137.6, 141.1, 144.5, 149.4, 155.3, 169.3. $\tilde{\nu}_{max}$/cm^{-1} 3468 (ν NH), 1749 (ν CO), 1635, 1502 (δ NH). UV-VIS (H_2O): λ_{max}/nm (ε_{max}/$M^{-1}cm^{-1}$), 256 (8.9×10^4), 362 (1.2×10^4), 381 (1.2×10^4).

[(η⁵-C_5Me_5)Ir(dppz)(9-Etgua)](CF_3SO_3)$_2$ 15. Method A, 18 h, 60 °C. Yield 111.5 mg, 79% (Found: C, 40.3; H, 3.5; N, 11.8; S, 5.4. Calc. for $C_{37}H_{33}F_6IrN_9O_7S_2$: C, 40.9; H, 3.1; N, 11.6; S, 5.9%). FAB mass spectrum: *m/z* 610.0 (100, [(η⁵-Cp*)Ir(dppz)]$^+$), 758.9 (20, [(η⁵-Cp*)Ir(dppz) + $[CF_3SO_3]^+$) and 938.0 (1%, $[M - CF_3SO_3]^+$). ^{1}H NMR (CD_3OD): δ 1.21 (t, 3H, Et), 1.80 (s, 15H, Cp*), 3.98 (q, 2H, Et), 7.87 (s, 1H H8,$_{gua}$), 8.13 (m, 2H), 8.46 (m, 4H), 9.94 (m, 4H). ^{13}C NMR (CD_3OD): δ 8.8 (Cp*), 15,5 (CH_3 Et), 41.1 (CH_2 Et), 93.3 (Cp*), 129.9, 131.1, 132.6, 133.9, 137.1, 141.0, 141.2 ($C_{8,gua}$), 144,5, 151.8, 153.8, 154.6, 156.3, 156.9. $\tilde{\nu}_{max}$/cm^{-1} 3338 (ν NH), 1705, 1639 (ν CO), 1578 (δ NH). UV-VIS (H_2O): λ_{max}/nm (ε_{max}/$M^{-1}cm^{-1}$), 280 (5.6×10^4), 363 (1.2×10^4), 382 (1.2×10^4).

[(η⁵-C_5Me_5)Ir(9-Etgua)(phen)](CF_3SO_3)$_2$ 16. Method A, 18 h, 60 °C. Yield 99.8 mg, 78% (Found: C, 37.6; H, 3.3; N, 10.4; S, 6.1. Calc. for $C_{31}H_{32}F_6IrN_7O_7S_2$: C, 37.8; H, 3.3; N, 9.9; S, 6.5%). FAB mass spectrum: *m/z* 507.9 (100, [(η⁵-Cp*)-Ir(phen)]$^+$), 656.8 (56, [(η⁵-Cp*)Ir(phen) + $[CF_3SO_3]^+$) and 835.9 (6%, $[M - CF_3SO_3]^+$). ^{1}H NMR (CD_3OD): δ 1.16 (t, 3H, Et), 1.77 (s, 15H, Cp*), 3.95 (q, 2H, Et), 7.70 (s, 1H, $H_{8,gua}$), 8.26 (s, 2H), 8.31 (m, 2H), 8.94 (dd, 2H), 9,92 (dd, 2H). ^{13}C NMR (CD_3OD): δ 8.8 (Cp*), 15.5 (CH_3 Et), 40.9 (CH_2 Et), 93.1 (Cp*), 128.7, 129.7, 132.9, 141.0, 141.9 ($C_{8,gua}$), 148.6, 153.4, 153.7, 155.4, 156.3, 156.8. $\tilde{\nu}_{max}$/cm^{-1} 3498 (ν NH), 1691, 1602 (ν CO), 1582 (δ NH). UV-VIS (H_2O): λ_{max}/nm (ε_{max}/$M^{-1}cm^{-1}$), 272 (3.0×10^4), 356 (0.2×10^4).

X-Ray crystallography

Unit-cell constants were obtained by least-squares refinement on centred angles for 25 reflections ($25 < 2\theta < 30°$) on a Siemens P4 diffractometer. Intensity data were collected at 293 K in the ω-scan mode with monochromated Mo-Kα radiation (λ = 0.71073 Å). Three control reflections were monitored after collection of 100 reflections and displayed no significant variations in intensity. The structures were solved by a combination of Patterson and Fourier-difference syntheses and refined by full-matrix least squares against F^2 using SHELXL.[29] Scattering factors and corrections for anomalous dispersion were taken from ref. 30.

Complex 3. $C_{29}H_{25}ClF_3IrN_4O_3S$, M = 794.2, triclinic, space group $P\bar{1}$ (no. 2), a = 8.299(2), b = 11.871(2), c = 15.606(3) Å, α = 73.98(1), β = 75.55(1), γ = 74.22(2)°, U = 1396.5(5) Å^3, Z = 2, D_c = 1.889 Mg m^{-3}, F(000) = 776, yellow prism with dimensions 0.35 × 0.18 × 0.16 mm, μ(Mo-Kα) = 5.01 mm^{-1}, 2θ data collection range 4–50°, ± h, ± k, ± l, 4873 independent reflections, 3854 of which with $I > 2\sigma(I)$, R1 = 0.039 [$I > 2\sigma(I)$], wR2 = 0.089 (all data), S (goodness-of-fit) = 0.899, max., min. $\Delta\rho$ = 1.26, −0.73 e Å^{-3}. All nonhydrogen atoms were assigned anisotropic temperature factors. H atoms were included at calculated positions.

Complex 16. $C_{31}H_{32}F_6IrN_7O_7S_2 \cdot 1.25CH_3OH$, M = 1025.01, triclinic, space group $P\bar{1}$ (no. 2), a = 12.755(3), b = 13.247(3), c = 14.711(7) Å, α = 63.27(3), β = 70.26(2), γ = 88.88(2)°, U = 2063.5(12) Å^3, Z = 2, D_c = 1.650 Mg m^{-3}, F(000) = 1017, yellow prism with dimensions 0.46 × 0.28 × 0.22 mm, μ(Mo-Kα) = 3.42 mm^{-1}, 2θ data collection range 4–50°, + h, ± k, ± l, 6896 independent reflections, 5969 of which with $I > 2\sigma(I)$, R1 = 0.046 [$I > 2\sigma(I)$], wR2 = 0.135 (all data), S (goodness-of-fit) = 1.101, max., min. $\Delta\rho$ = 2.08, −2.29 e Å^{-3}. The asymmetric unit contains three disordered methanol molecules. All other non-hydrogen atoms were assigned anisotropic temperature factors; with the exception of the CH_3OH molecules, H atoms were included at calculated positions.

CCDC reference numbers 173003 and 173004.

See http://www.rsc.org/suppdata/dt/b1/b107656f/ for crystallographic data in CIF or other electronic format.

References

1 A. E. Friedman, J. Chambron, J. Sauvage, N. J. Turro and J. K. Barton, *J. Am. Chem. Soc.*, 1990, **112**, 4960.
2 B. Nordén, P. Lincoln, B. Åkerman and E. Tuite, *Metal Ions in Biological Systems*, eds. A. Sigel and H. Sigel, Marcel Dekker, New York, 1996, vol. 33, p. 177.
3 K. E. Erkkila, D. T. Odom and J. K. Barton, *Chem. Rev.*, 1999, **99**, 2777.
4 T. K. Schoch, J. L. Hubbard, C. R. Zoch, G.-B. Yi and M. Sørlie, *Inorg. Chem.*, 1996, **35**, 4383.
5 W. S. Sheldrick and A. J. Gleichmann, *J. Organomet. Chem.*, 1994, **470**, 183.
6 W. S. Sheldrick and S. Heeb, *Inorg. Chim. Acta*, 1998, **168**, 93.
7 W. S. Sheldrick and S. Heeb, *J. Organomet. Chem.*, 1989, **377**, 357.
8 R. Krämer, K. Polborn, H. Wanjek, I. Zahn and W. Beck, *Chem. Ber.*, 1990, **123**, 127.
9 K. Severin, R. Bergs and W. Beck, *Angew. Chem., Int. Ed.*, 1998, **37**, 1634.
10 D. Carmona, F. J. Lahoz, R. Atencio, L. A. Oro, M. Pilar Lamata, F. Viguri, E. San José, C. Vega, J. Reyes, F. Joó and A. Kathó, *Chem. Eur. J.*, 1999, **5**, 1544.
11 J. Sartorius and H.-J. Schneider, *FEBS Lett.*, 1995, **374**, 387.
12 J. Sartorius and H.-J. Schneider, *J. Chem. Soc., Perkin Trans. 2*, 1997, 2319.
13 N. Y. Sardesai, K. Zimmermann and J. K. Barton, *J. Am. Chem. Soc.*, 1994, **116**, 7502.
14 A. M. Pyle, J. P. Rehmann, R. Meshoyrer, C. V. Kumar, N. J. Turro and J. K. Barton, *J. Am. Chem. Soc.*, 1989, **111**, 3051.

15 M. T. Carter, M. Rodriguez and A. J. Bard, *J. Am. Chem. Soc.*, 1989, **111**, 8901.
16 S. R. Smith, G. A. Neyhart, W. A. Karlsbeck and H. H. Thorp, *New J. Chem.*, 1994, **18**, 397.
17 S. Moghaddas, P. Hendry, R. J. Geue, C. Qin, A. M. T. Bygott, A. M. Sargeson and N. E. Dixon, *J. Chem. Soc., Dalton Trans.*, 2000, 2085.
18 C. V. Kumar and E. H. Asuncion, *J. Chem. Soc., Chem. Commun.*, 1992, 470.
19 C. M. Dupureur and J. K. Barton, *J. Am. Chem. Soc.*, 1994, **116**, 10286.
20 C. M. Dupureur and J. K. Barton, *Inorg. Chem.*, 1997, **36**, 33.
21 I. Greguric, J. R. Aldrich-Wright and J. G. Collins, *J. Am. Chem. Soc.*, 1997, **119**, 3621.
22 J. G. Collins, A. D. Sleeman, J. R. Aldrich-Wright, I. Greguric and T. W. Hambley, *Inorg. Chem.*, 1998, **37**, 3133.
23 C. White, S. J. Thompson and P. M. Maitlis, *J. Organomet. Chem.*, 1977, **127**, 415.
24 C. White, S. J. Thompson and P. M. Maitlis, *J. Chem. Soc., Dalton Trans.*, 1977, 1654.
25 J. E. Dickeson and L. A. Summers, *Aust. J. Chem.*, 1970, **23**, 1023.
26 M. Yamada, Y. Tamaka and Y. Yashimoto, *Bull. Chem. Soc. Jpn.*, 1992, **65**, 1006.
27 H.-Q. Liu, T. C. Cheng, S.-M. Peng and C.-M. Che, *J. Chem. Soc., Chem. Commun.*, 1995, 1787.
28 J. Marmur, *J. Mol. Biol.*, 1961, **3**, 208.
29 G. M. Sheldrick, SHELX-97 programs for structure solution and refinement, Göttingen, Germany, 1997.
30 *International Tables for X-Ray Crystallography*, Kynoch Press, Birmingham, 1971, vol. 4.